Appl. Magn. Reson. (2008) 35, 221–230
DOI 10.1007/s00723-008-0156-y
Printed in The Netherlands

Applied
Magnetic Resonance

In Situ Conduction ESR and Theoretical Studies of Graphite Intercalation by Antimony Pentafluoride*

A. M. Ziatdinov, A. G. Sviridova, V. V. Sereda, and **P. G. Skrylnik**

Institute of Chemistry, Russian Academy of Sciences, Vladivostok, Russian Federation

Received 25 August 2006; revised 28 February 2008
© Springer-Verlag 2008

Abstract. The results of an in situ conduction electron spin resonance (CESR) study of the intercalation of SbF_5 molecules into highly oriented pyrolytic graphite are presented. The narrowing (broadening) of the CESR signal from intercalated (nonintercalated) parts of the graphite plate during advance of the reaction front into graphite is explained by the nonzero probability of the spin reorientation at collisions of current carriers with the intercalation front and by a decrease (increase) of frequency of these collisions. The assumption was made that the stepwise increase in the intensity of the CESR signal from intercalated parts of the graphite plate during the reaction is due to the presence of an intercalation threshold and periodical impoverishing of the adsorbed layers of the intercalant. The results of calculations conducted within the framework of this model fit the experimental data well.

1 Introduction

Graphite intercalation compounds (GICs) form a large family of the layered intercalation compounds. The intercalation process and staging phenomena in GICs have been in the focus of attention of researchers for a long time [1, 2].

The conduction electron spin resonance (CESR) technique is one of the most powerful methods for studying the graphite intercalation process because shapes and intensities of the CESR signal from both nonintercalated and intercalated regions of the graphite plate vary significantly during intercalation. However, because of the difficulty to conduct reproducible experiments, only a few CESR studies of the graphite intercalation process have been undertaken [3–8].

This paper is devoted to the results of an in situ CESR study of the intercalation of antimony pentafluoride (SbF_5) molecules into highly oriented pyrolytic graphite (HOPG) plates with a width being comparable with or much larger than

* Presented at the 5th Asia-Pasific EPR/ESR Symposium, August 24–27, 2006, Novosibirsk, Russian Federation.

the skin depth, δ_c, governed by the *c*-axis conductivity σ_c. The experiments clearly show the stepwise nature of the intercalation and large spin relaxation probability at collisions of current carriers with the intercalation front.

2 Experimental

CESR measurements were carried out at room temperature using an X-band E-line spectrometer. The experiments were conducted on HOPG plates with height (h), width (l) and thickness (d) being 0.4, 0.032 and 0.034 cm, respectively, for sample A and 0.94, 0.58 and 0.035 cm, respectively, for sample B, with lh defining the size of the basal plane. During measurements, the constant magnetic field H_0 was applied along the graphite *c*-axis and perpendicular to the magnetic component of the microwave field H_{rf}. It is worth noting that in the rectangular resonator the structure of the electromagnetic field of the TE_{102} mode has such a form that at conventional settings of the resonator, H_0 is parallel to the electrical component, E_{rf}, of the microwave field.

The HOPG samples were held in a quartz tube connected via a valve to the reservoir with intercalant (at standard conditions, SbF_5 is a colorless liquid with a density of 2.99 g/cm^3, melting point of +7 °C, boiling point of +150 °C, vapor pressure of about 1 Torr [ca. 100 Pa]). SbF_5 vapor penetrated into the knee of the reactor with the graphite sample through the $5 \cdot 10^{-2}$ cm^2 hole in the fluoroplastic diaphragm. Prior to the experiment, the system was evacuated to eliminate water vapor.

In situ measurements of the conductivity σ_a^* along the basal plane of the (HOPG plus SbF_5) system versus the time of exposure in the SbF_5 vapor were carried out on the B-type sample by a contactless method analogous to that described in ref. 9. According to data of the four-probe method, at 300 K the σ_c conductivity of the HOPG plate used is equal to about 7.7 $\Omega^{-1} \cdot cm^{-1}$. In X-band the value $\delta_c \approx l_A/2$ (l_A is the width of sample A) corresponds to this conductivity, i.e., the whole volume of sample A was available for CESR studies.

The stage of the compound in intercalated parts of the HOPG plate was determined by X-ray diffraction (XRD) method.

3 Results

The CESR spectrum for both HOPG plates investigated consists of a single asymmetric line determined by the Dyson mechanism [10]. The spectrum is axial with respect to the *c*-axis. The principal values of the *g*-factor, g_c and g_a, determined by Feher–Kip procedure [11] are equal to 2.0474 ± 0.0001 and 2.0029 ± 0.0001 for $H_0 \parallel c$ and $H_0 \perp c$, respectively. For CESR spectra at $H_0 \parallel c$ the line shape asymmetry parameter, A/B (determined as the maximum-to-minimum peak height ratio, measured with respect to the baseline of the first derivative of the CESR absorption line), is about 2.3 and 4 for samples A and B, respectively. Therefore, for sample B ($l \gg \delta_c$) the value of A/B is essentially metallic. The small value

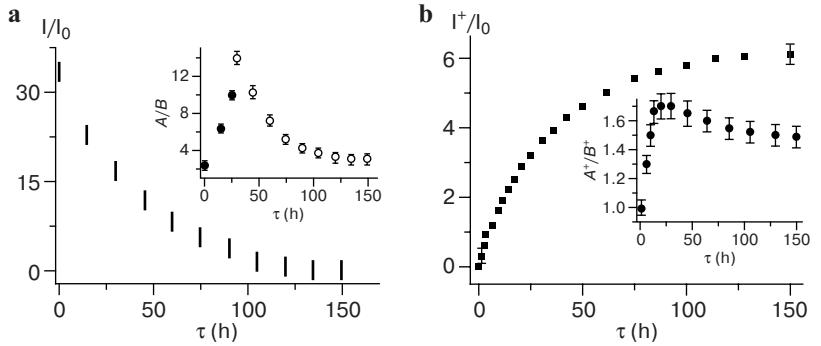

Fig. 1. CESR signal parameters I, I^+, A, B, A^+ and B^+ of nonintercalated (**a**) and intercalated (**b**) parts of the HOPG plate (sample A) versus the exposure time τ in SbF_5 atmosphere. I_0 is the intensity of the standard ESR signal. $c \parallel H_0$, $c \perp H_{rf}$, $T = 300$ K.

of A/B for the graphite plate A ($l \approx 1.6\delta_c$) can be explained by the fact that the CESR line shape tends to the Lorentzian one with $A/B = 1$ at $l \to 0$.

After the induction time of the reaction (about 10 min), the CESR signal of graphite begins to transform and its intensity parameter I ($I = (A + B)\Delta H^2$, where ΔH is the line width at the half-height of the A peak), monotonously decreases versus the exposure time τ until it fully disappears (Fig. 1a). At the same time a new signal with $g_c^+ = 2.0021 \pm 0.0001$ and $g_a^+ = 2.0027 \pm 0.0001$ appears in the spectrum. The intensity parameter of this signal I^+ ($I^+ = (A^+ + B^+)\Delta H^{+2}$, where A^+, B^+ and ΔH^+ are the line shape parameters analogous to A, B and ΔH) monotonously increases with exposure time (Fig. 1b). Simultaneously, the line width of this signal monotonously decreases (Fig. 2a) and that of graphite increases

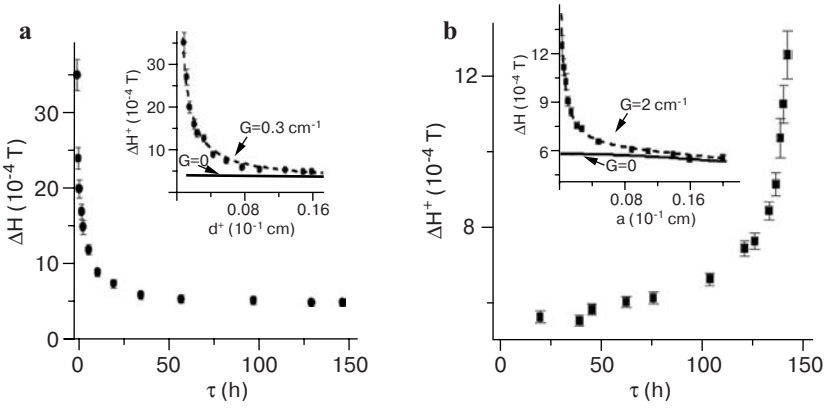

Fig. 2. Line width of the CESR signal from intercalated (**a**) and nonintercalated (**b**) parts of the HOPG plate (sample A) versus the exposure time τ in SbF_5 atmosphere. The experimental (dots) and theoretical (dotted line) values of the line width versus the thickness of intercalated (d^+) and nonintercalated ($a = l_A - 2d^+$) parts of graphite are presented in the corresponding insets. $c \parallel H_0$, $c \perp H_{rf}$, $T = 300$ K.

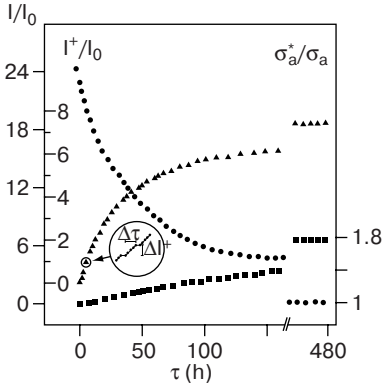

Fig. 3. Intensity of the CESR signal from intercalated I^+/I_0 (▲) and nonintercalated I/I_0 (●) parts and conductivity σ_a^+ (■) of the HOPG plate (sample B) versus the exposure time τ in SbF_5 atmosphere. σ_a is the graphite basal-plane conductivity and I_0 is the intensity of the standard ESR signal. $c \parallel H_0$, $c \perp H_{rf}$, $T = 300$ K.

(Fig. 2b). The values of g_i and g_i^+ ($i = a, c$) remain constant up to the end of intercalation.

At the beginning of the reaction the A/B ratio of the graphite CESR signal increases, but it is still normal reaching a maximum value $A/B \approx 14$ (Fig. 1a). Later, upon further exposure in the intercalant atmosphere, the A/B ratio becomes reversed (the maximum peak height A occurs at higher magnetic fields than the smaller peak B), and its magnitude decreases to a value of about 3; the A/B maximum corresponds to the moment when the reversal of the CESR line shape takes place (Fig. 1a). For sample B, the evolution of the CESR line shape asymmetry ratio for the graphite signal is qualitatively the same as for sample A.

For sample B for any orientation of the c-axis relative to H_0, the $I^+(\tau)$ dependence takes a well-marked stepped form from the very appearance of this signal in the spectrum (Fig. 3). It consists of a number of small steps, representing the sequence of alternating sections with different slope values (Fig. 3). With increasing exposure time, the step length $\Delta\tau$ increases, while its height ΔI^+ decreases. However, both parameters vary slowly enough to choose time intervals containing almost identical steps. For sample A the stepwise changes in the intensity of the CESR signal with g_i^+ ($i = a, c$) were not observed (Fig. 1b).

4 Discussion

In traditional configuration of the ESR experiment the microwave field penetrates into the HOPG plate mainly through its lateral sides, which are simultaneously parallel to both the c-axis and H_{rf} [12]; in our case through the lateral sides hd. Therefore, the evolution of the graphite CESR signal for the samples investigated (Figs. 1a, 2b and 3) is mainly due to variations of the composition and proper-

ties of the HOPG plate at surface areas with the thickness of about δ_c from these sides due to the diffusion of SbF_5 molecules into graphite. The dependences of the shape and intensity of the graphite CESR signal on the exposure time are qualitatively identical to those of the CESR signal line shape and intensity of the conductive substrate on the thickness of a spray-coated film of another metal [13]. In our case, the spins in consideration are certainly mobile but in sample A ($l/\delta_c < 2$) the CESR line shape does not depend on the spin mobility [14], i.e., in the framework of the Dyson theory [10] spin carriers may be considered as localized. Therefore, variations of the shape and intensity of the graphite CESR signal in sample A (Fig. 2b) may be due to the formation of a macroscopic intercalation layer on the HOPG plate (with a conductivity different from that of initial material) and advance of the interface separating this layer from as-yet nonintercalated parts of the sample (due to diffusion of antimony pentafluoride molecules into the graphite along its galleries). By taking into account that changes in the line shapes and intensities of the graphite CESR signals at intercalation are qualitatively identical for samples A and B, one may assume a common origin for these changes.

The invariability of *g*-factor values for CESR spectra from nonintercalated and intercalated areas of the graphite plate until disappearance of the graphite CESR signal and the end of experiment, respectively, indicates that the frequency of transitions of current carriers between them is much less than the microwave frequency. An interface barrier apparently appears as a result of significant distortions of the carbon net in the direction through the intercalation front (the distance between the nearest carbon layers in initial graphite and in its intercalation compounds with SbF_5 is equal to 0.335 and 0.846 nm [1], respectively). The existence of such a barrier in the HOPG-plus-SbF_5 system is also confirmed by analysis of CESR spectra from plates obtained by cutting the partially intercalated samples in different manners. In particular, this is confirmed by observation of the graphite CESR signal (with the same parameters as for initial whole graphite plate) from halves of plate B exposed to SbF_5 vapors until disappearance of the graphite CESR spectrum before cutting.

In the experiment with sample A the whole plate volume is available for CESR investigation. Therefore, in this case we have good reason to believe that the time of disappearance of the graphite CESR signal corresponds to the moment of contact of two counter (antiparallel) intercalation fronts. By assuming that graphite intercalation with antimony pentafluoride molecules is a two-dimensional (2-D) diffusion process, it is easy to estimate the parameter of 2-D intercalant diffusion $D_{int} \approx 2.4 \cdot 10^{-10}$ cm^2/s by substituting the value of the time interval $\Delta\tau$ from the beginning of the graphite CESR signal transformation up to its disappearance (Fig. 1a) instead of $\Delta\tau$, and setting $\Delta x = l_A/2$ into the expression $\Delta x = (2D_{int}\Delta t)^{1/2}$.

An unexpected result of our experiments is the significant narrowing of the CESR signal from intercalated regions at the beginning of the reaction (Fig. 2a) and the significant broadening of the graphite CESR signal before the contact of the counter intercalation fronts (Fig. 2b). The presence of significant distortions of the carbon net in the direction through the intercalation front and its advance into the graphite slab with increasing exposure time allow to consider

both unusual line shape dependences as caused by collisions of current carriers with the moving interface between nonintercalated and intercalated parts of the sample.

Using the relation $d^{+2} = 2D_{\text{int}}\tau$ (d^+ is the average thickness of the intercalated layer), the experimental dependence $\Delta H(\tau)$ can be easily transformed into the dependence $\Delta H(a)$, where $a = l_A - 2d^+$ is the thickness of the nonintercalated part of HOPG (Fig. 2b, inset). The latter dependence can be calculated theoretically as well, using the extended Dyson expressions for CESR in metals including the effects of surface spin relaxation [10]. From the inset of Fig. 2b, where the results of such calculations are presented for sample A, it can be seen that the theoretical dependence of the graphite CESR line width with a nonzero value of the Dyson surface spin-relaxation parameter $G = 3\varepsilon/4\Lambda$ (ε is the average surface spin reorientation probability, Λ is the mean free path of current carriers) fits the experimental data well. The found value of $G \equiv G_a = 2$ cm^{-1} (G_a is the average graphite–intercalant interface spin-relaxation parameter) and typical HOPG values of mean free path of current carriers in the basal plane $\Lambda_a \approx 7.7 \cdot 10^{-6}$ cm [15] correspond to the average graphite–intercalant interface spin reorientation probability $\varepsilon \equiv \varepsilon_a \approx 2 \cdot 10^{-5}$.

Application of the above technique to the analysis of $\Delta H^+(d^+)$ dependence (Fig. 2a, inset) gives the value of average intercalant–graphite interface spin-relaxation parameter $G \equiv G_a = 0.3$ cm^{-1}. Therefore, the value of G_a^+ is about 7 times smaller than the value of G_a. We believe that the reason(s) for this discrepancy may be the strong spin-relaxation of current carriers at their collisions with the GIC surface and/or the asymmetry of magnetic interactions for current carriers swooping on the intercalation front from the graphite and GIC sides.

Dependences of I^+ on the time of exposure in SbF_5 vapors for sample B have a stepped shape (Fig. 3). However, different from similar dependences observed in previous experiments with nitric acid GIC [7, 8], in this case the stepped character of $I^+(\tau)$ dependences is not due to transitions between different GIC stages (stage transitions). Indeed, XRD data of the HOPG-plus-SbF_5 system obtained at different times of the intercalation process demonstrate that XRD spectra at any time contain only first stage SbF_5-GIC reflections of increasing intensity and pristine graphite reflections of decreasing intensity. Therefore, at theoretical analysis of stepwise $I^+(\tau)$ dependence (Fig. 3), models for nitric acid molecules intercalation into graphite, based on the previously developed concept of stage transitions in GICs [8], are not applicable. Therefore, these data have been analyzed within the framework of an essentially different physical model presented below.

It is well known [16] that the CESR signal intensity is proportional to the density of states at the Fermi level. Within the framework of a rigid band model for acceptor GICs this density of states is proportional to the charge transferred from the carbon net to the intercalant [1]. In turn, the latter is approximately proportional to the number of guest molecules inserted into graphite [1]. Taking into account the above consideration, one may assume that in this experiment the stepped character of the $I^+(\tau)$ dependence reflects the discontinuous character of the process of antimony pentafluoride intercalation into graphite,

where intercalant inserts graphite galleries by portions within the same growing GIC stage.

In the experiment with sample B the intervals of fast increase in the intensity of the CESR signal from intercalated graphite areas may be attributed to the phase of reaction, concerned with the absorption of intercalant and subsequent intercalation front proceeding along the graphite galleries to the center of the sample. Evidently, this process is ceased when the intercalant concentration on outer faces of the sample decreases below a certain threshold value (lower threshold of the reaction). Therefore, the next phase of reaction corresponding to the plateau region in the $I^+(\tau)$ dependence (Fig. 3) may be attributed to the phase of accumulation of intercalant on the faces up to the amount sufficient to exceed the intercalation threshold (upper threshold of intercalation). It is worth mentioning that the presence of upper and lower intercalation thresholds does not contradict to the general physical concepts.

According to the presented ideas, the physical reason for the portional intercalation into the graphite plate is a competition of two different periodical processes: accumulation of the adsorbed intercalant molecules on the sample faces up to the threshold concentration necessary for intercalation to begin, followed by subsequent decrease in this concentration resulting from intercalation of part of molecules from surfaces deep into graphite galleries. Such decrease continues down to some concentration value and intercalation is almost impossible below this threshold.

The absence of any steps in the $I^+(\tau)$ dependence for the narrow sample A (Fig. 1b) shows that in this sample the time interval of intercalant accumulation on its outer surfaces is small or absent at all. The possible reasons for that may be the much smaller amount of intercalant molecules necessary for beginning of the insertion or/and the lower intercalation threshold due to greater heating of a thin sample in the microwave field of the resonator.

For the analysis of experimental dependences of the CESR signal intensity versus time for the HOPG plate during SbF_5 intercalation, calculations within the framework of the following model have been conducted.

The intercalation process consists of a sequence of repeating phases of two types: accumulation of the intercalant on the sample surface (phase I) and immediate intercalation (phase II). The accumulation process is of saturation nature and in the simple case its rate is proportional to $(S_m - S)$, where $S - S(\tau)$ is the intercalant concentration on the surface, S_m is the limiting value corresponding to saturation. The rate of immediate intercalation process is proportional to the concentration of accumulated intercalant S. Therefore, in the simple case the phenomenon under investigation may be described with a system of differential equations for $S(\tau)$ and intercalant concentration inside the sample $C(\tau)$:

$$dS/d\tau = \alpha(S_m - S) - \beta SP, \quad \text{and} \quad dC/d\tau = \beta SP,$$

where α is the parameter determining the rate of intercalant accumulation on the surface (it depends on the intercalant type, intercalant vapor pressure, surface of

the sample, temperature, etc.), β the parameter determining the insertion rate (depends on the intercalant type, degree of the structure imperfection of initial sample, temperature, etc.), $P = 0$ for phase I and $P = 1$ for phase II. The solutions of this simple system are as follows:

for phase I,

$$S(\tau) = S_m - (S_m - S_0)\exp(-\alpha\tau),$$

$$C(\tau) = C_0;$$

for phase II,

$$S(\tau) = S_0\Omega + \frac{\alpha S_m}{(\alpha+\beta)}(1-\Omega),$$

$$C(\tau) = C_0 + \frac{\beta S_0}{(\alpha+\beta)}(1-\Omega) + \frac{\alpha\beta S_m}{(\alpha+\beta)^2}((\alpha+\beta)\tau + \Omega - 1),$$

$$\Omega = \exp(-(\alpha+\beta)\tau).$$

The time origin is at the beginning of the particular phase, therefore $S_0 = S(0)$ and $C_0 = C(0)$ correspond to the concentration values reached at the beginning of the particular phase. Criterion for transition from the accumulation phase to the phase of intercalation and, further, to the next accumulation phase is the reaching of the upper threshold concentration value S_1 and of the lower threshold value S_2, respectively.

We believe that their magnitudes should be determined by the amount of already inserted intercalant C, for instance, as follows:

$$S_1 = C + \mu + \eta, \text{ and } S_2 = C + \mu.$$

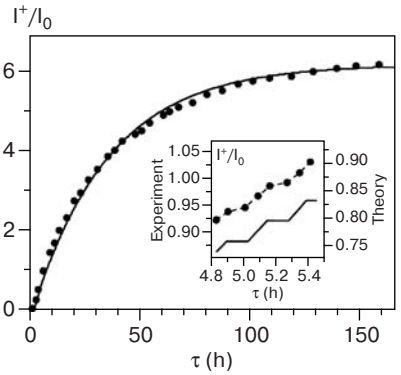

Fig. 4. Comparison of the experimental dependence $I^+(\tau)$ (dots) and the calculated one (solid line) for sample B. Inset presents the structure of these dependences.

In this case μ is equal to the value of S_2 at the beginning of reaction and the difference $(S_1 - S_2)$ is constant and equal to η. The calculations conducted within the framework of the presented model have demonstrated that a qualitatively good description of the experimental $I^+(\tau)$ dependence (supposing $I^+(\tau) \sim C(\tau)$) may be reached at the following set of parameters: $\alpha = 1.569 \cdot 10^{-5}$ s^{-1}, $\beta = 1.0 \cdot 10^{-4}$ s^{-1}, $\mu = 0.1$, $\eta = 0.04$, $S_m = 6.3$ (parameters μ, η and S_m are expressed in arbitrary units). The results of calculations are presented in Fig. 4. It is clear that though the calculation model is simplified, it depicts main features of experimental data, and the calculated curve describes the experimental dependence qualitatively well.

5 Conclusion

Graphite intercalation by SbF_5 molecules has been studied by the CESR technique in HOPG plates with widths being much larger or comparable with the graphite skin depth governed by the *c*-axis conductivity. As a result, a significant narrowing (broadening) of the GIC (graphite) CESR signal during transport of the intercalant through the initial graphite sample and stepwise changes in the intensity of the intercalated graphite CESR signal versus the exposure time in SbF_5 atmosphere have been clearly detected. The narrowing (broadening) of the GIC (graphite) CESR signal during the advance of the intercalation front into the initial graphite sample is explained by the nonzero probability of the spin reorientation during collisions of current carriers with the interface between the intercalated and the nonintercalated parts of the plate. The assumption was made that the reasons for the partial insertion of intercalant are the presence of an upper intercalation threshold (intercalation into the sample becomes permitted above this value) and a lower threshold (intercalation is almost impossible below it) and the periodical impoverishing of intercalant molecule layers adsorbed on graphite. Presented model calculations have resulted in a qualitatively good description of the experimental dependences. Similar experimental and theoretical investigations of graphite intercalation by other intercalants are in progress.

Acknowledgments

We are grateful to N. M. Mishchenko for help in experiments, L. B. Nepomnyashchii (Scientific Research Center for Graphite, Moscow) and A. K. Tsvetnikov for providing us with HOPG and SbF_5, respectively. This work was supported by the Russian Foundation for Basic Research (grant nr. 04-03-32135).

References

1. Dresselhaus, M.S., Dresselhaus, G.: Adv. Phys. **30**, 139–326 (1981)
2. Solin, S.A., Zabel, H.: Adv. Phys. **37**, 87–254 (1988)
3. Davidov, R., Milo, O., Palchan, I., Selig, H.: Synth. Met. **8**, 83–87 (1983)

4. Palchan, I., Davidov, D., Zevin, V., Polatsek, G., Selig, H.: Synth. Met. **12**, 413–418 (1985)
5. Palchan, I., Mustachi, F., Davidov, D., Selig, H.: Synth. Met. **10**, 101–106 (1984/1985)
6. Nakajima, M., Kawamura, K., Tsuzuku, T.: J. Phys. Soc. Jpn. **57**, 1572–1575 (1988)
7. Ziatdinov, A.M., Mishchenko, N.M.: J. Phys. Chem. Solids **58**, 1167–1172 (1997)
8. Ziatdinov, A.M., Skrylnik, P.G.: Chem. Phys. **261**, 439–448 (2000)
9. Zeller, C., Foley, G.M.T., Falardeau, E.R., Vogel, F.L.: Mater. Sci. Eng. **31**, 255–259 (1977)
10. Dyson, F.J.: Phys. Rev. **98**, 349–359 (1955)
11. Feher, G., Kip, A.F.: Phys. Rev. **98**, 337–348 (1955)
12. Ziatdinov, A.M., Mishchenko, N.M.: Fiz. Tverd. Tela (St. Petersburg) **36**, 1283–1289 (1994)
13. Zevin, V., Suss, J.T.: Phys. Rev. B. **34**, 7260–7270 (1986)
14. Kodera, H.J.: Phys. Soc. Jpn. **28**, 89–98 (1970)
15. Spain, J.L., in: Walker, P.L. (ed.) Chemistry and Physics of Carbon, vol. 8, pp. 119–305. Marcel Dekker, New York (1973)
16. Winter, J.: Magnetic Resonance in Metals, p. 121. Clarendon, Oxford (1971)

Authors' address: Albert M. Ziatdinov, Institute of Chemistry, Russian Academy of Sciences, prospect 100-letiya Vladivostoka 159, 690022 Vladivostok, Russian Federation
E-mail: ziatdinov@ich.dvo.ru